A Role for the Frontal Aslant Tract in Speech Planning: A Neurosurgical Case Study

Benjamin L. Chernoff[1], Alex Teghipco[1], Frank E. Garcea[1], Max H. Sims[1], David A. Paul[2], Madalina E. Tivarus[2], Susan O. Smith[2], Webster H. Pilcher[2], and Bradford Z. Mahon[1,2]

Abstract

■ Frontal and temporal white matter pathways play key roles in language processing, but the specific computations supported by different tracts remain a matter of study. A role in speech planning has been proposed for a recently described pathway, the frontal aslant tract (FAT), which connects the posterior inferior frontal gyrus to the pre-SMA. Here, we use longitudinal functional and structural MRI and behavioral testing to evaluate the behavioral consequences of a lesion to the left FAT that was incurred during surgical resection of a frontal glioma in a 60-year-old woman, Patient AF. The pattern of performance in AF is compared, using the same measures, with that in a 37-year-old individual who underwent a left anterior temporal resection and hippocampectomy (Patient AG). AF and AG were both cognitively intact preoperatively but exhibited specific and doubly dissociable behavioral deficits postoperatively: AF had dysfluent speech but no word finding difficulty, whereas AG had word finding difficulty but otherwise fluent speech. Probabilistic tractography showed that the left FAT was lesioned postoperatively in AF (but not AG) whereas the inferior longitudinal fasciculus was lesioned in AG (but not AF). Those structural changes were supported by corresponding changes in functional connectivity to the posterior inferior frontal gyrus: decreased functional connectivity postoperatively between the posterior inferior frontal gyrus and pre-SMA in AF (but not AG) and decreased functional connectivity between the posterior inferior frontal gyrus and the middle temporal gyrus in AG (but not AF). We suggest from these findings that the left FAT serves as a key communicative link between sentence planning and lexical access processes. ■

INTRODUCTION

The frontal aslant tract (FAT) consists of white matter fibers that connect the pre-SMA to the ACC and the posterior inferior frontal gyrus. The anatomy of this white matter tract has been described in human diffusion tensor imaging (DTI) tractography studies (Mandelli et al., 2014; Catani et al., 2012, 2013; Ford, McGregor, Case, Crosson, & White, 2010), human postmortem dissection (Lawes et al., 2008), and nonhuman primate tractography studies (Thiebaut de Schotten, Dell'Acqua, Valabregue, & Catani, 2012). The anatomy of the FAT suggests an important role for this pathway in speech production, and this expectation has been borne out by studies of the functional consequences of damage to the FAT. Patients with primary progressive aphasia have been found to have verbal fluency deficits that correlate with fractional anisotropy (FA) and radial diffusivity (RD) in the FAT, but not other tracts underpinning language function (Mandelli et al., 2014; Catani et al., 2013). Another line of research on the FAT emphasizes its role in stuttering, developmentally and also in adulthood. Kronfeld-Duenias, Amir, Ezrati-Vinacour, Civier, and Ben-Shachar (2016) found increased diffusivity in the left FAT as well as the corticospinal tract in adults who stutter compared with neurotypical controls. However, an inverse relation between diffusivity and speech rate was observed only in the left FAT (for other work on the corticospinal and corticobulbar tracts, see Cai et al., 2014; Dick, Bernal, & Tremblay, 2014; Chang, Erickson, Ambrose, Hasegawa-Johnson, & Ludlow, 2008). Direct current stimulation of left FAT intraoperatively in awake neurosurgery patients has been shown to cause intraoperative stuttering (Kemerdere et al., 2016) and speech arrest (Vassal, Boutet, Lemaire, & Nuti, 2014). In studies comparing postoperative damage to the FAT versus the more medial fronto-striatal tract, damage to the FAT is associated with transient speech initiation disorder, whereas damage to the frontal striatal tract is associated with difficulty initiating voluntary limb movements (Fujii et al., 2015; Kinoshita et al., 2014). Sierpowska and colleagues (2015) reported a case of a patient with a left premotor cortex tumor who completed a verb generation task during intraoperative electrical stimulation. The patient was able to execute the task when cortical areas were stimulated, but the patient made errors when subcortical structures, including or adjacent to the FAT, were stimulated.

At the cortical level, the superior termination of the FAT is in the SMA (Catani et al., 2012). Connectivity-based

[1]University of Rochester, [2]University of Rochester Medical Center

Journal of Cognitive Neuroscience 30:5, pp. 752–769
doi:10.1162/jocn_a_01244

parcellation using diffusion tractography (Klein et al., 2007) and functional connectivity (Kim et al., 2010) has dissociated the anterior portion of the SMA (pre-SMA) from the posterior portion of SMA (sometimes referred to as SMA proper). Although the pre-SMA and SMA proper are both associated with speech production, neuropsychological data suggest that the two regions may provide separate contributions. Hiroshima, Anei, Murakami, and Kamada (2014) studied 24 patients with lesions to the medial superior frontal gyrus preoperatively and postoperatively, as well as 32 healthy controls. Preoperative neuroimaging involved finger tapping, lexical decision, and verb generation. The language-related tasks consistently produced stronger activity in the pre-SMA than the right finger-tapping task, whereas finger tapping (both hands) was more associated with activity in the more posterior SMA proper. During surgery, stimulation of the finger tapping area of SMA produced contralateral hemiparesis with no language deficit. Stimulation of the language regions produced simple speech arrest and dysarthria (Hiroshima et al., 2014). Rozanski, Peraud, and Noachtar (2015) reported the case of a 44-year-old epileptic patient who had subdural grid and strip electrodes placed preoperatively to locate the foci of her epilepsy. Stimulation of posterior electrodes induced after-discharges and oral/facial cloni. Stimulation of the more anterior electrode in pre-SMA resulted in a speech production deficit whereby the patient could produce the preamble (e.g., "this is a" but could not name the object). After surgery in which the resection spared the primary motor regions, the patient had a mild speech initiation problem but no motor deficit.

Here, we present a case study of an individual with a left frontal glioma just anterior to the primary motor cortex and just superior to the inferior frontal gyrus. The patient underwent preoperative functional MRI for localization of language and awake cortical mapping during the surgery. Despite the resection avoiding eloquent cortical areas (defined by intraoperative language mapping), the patient presented with difficulties initiating speech after surgery. Preoperative and postoperative reconstruction of the FAT indicated that the integrity of this white matter pathway was affected by resection of the tumor and that functional connectivity between the pre-SMA and the posterior inferior frontal gyrus was reduced after surgery. We compare the MRI and behavioral measures obtained in this patient with those from a second patient who underwent resection of the left anterior temporal lobe (ATL) to access a hippocampal tumor. The comparison of a patient with surgery adjacent to the FAT with a patient who underwent left ATL resection is valuable because structural connectivity to the left inferior frontal gyrus from the temporal lobe is subserved via the uncinate fasciculus, which connects anterior mesial temporal to OFC and inferior frontal cortex. Inputs to the ATL from the occipital lobe come via the inferior longitudinal fasciculus (ILF), which connects occipital regions with the temporal pole (Catani, Howard, Pajevic, & Jones, 2002). Thus, our DTI investigation focuses on defining the FAT in both patients and the ILF in the patient who underwent the ATL resection. This allows us to dissociate the effects of lesions to the FAT (connecting the posterior inferior frontal gyrus to SMAs) from lesions to the inferior longitudinal fasciculus (communicating between the inferior frontal gyrus, via the uncinate fasciculus, and temporal regions involved in lexical semantic processing and lexical access).

METHODS

Participants

Patient AF is a right-handed 60-year-old woman who underwent surgery to remove a left frontal glioma in 2012. Before her surgery, AF was an author and a poet. After surgery, she began teaching a poetry class at a local college to aphasic individuals; she also continues with her artistic endeavors, although in her words, after surgery, she "lost her muse." She holds an Associate's degree (2-year undergraduate degree) and a Bachelor's degree, and her native language is English. The tumor was first discovered in 1992; AF, in consultation with her clinical team, decided at the time to wait and observe the tumor. In 2012, AF decided to move forward with an awake resection. Before her surgery, she completed a series of MRI (DTI, fMRI) and neuropsychological studies. She completed the same tests (some multiple times) postoperatively as well. Patient AG is a right-handed 37-year-old woman who underwent an awake resection of the left hippocampus and ATL. Before her surgery as well as after, she worked/s as a nurse. She holds an Associate's degree, and her native language is English. Both patients gave their written consent in accordance with the policies of the research subjects review board of the University of Rochester.

Neuropsychological Tests

Both patients were evaluated preoperatively and postoperatively to broadly assess language, praxis, visual processing, memory, and attention. All testing was video and/or audio recorded for offline analysis (for a detailed descriptions of the testing, see Stasenko, Garcea, Dombovy, & Mahon, 2014; Garcea, Dombovy, & Mahon, 2013). While we conducted a large array of tests as part of a standard battery for a broader longitudinal study in our laboratory, the current investigation is more narrowly focused around two measures of language ability: verbal fluency and picture naming.

Verbal Fluency

We were interested in assessing the integrity of "verbal fluency" due to the proximity of Patient AF's lesion to the superior and inferior frontal gyri. The posterior inferior frontal gyrus is classically involved in speech production,

and damage to the posterior inferior frontal gyrus is associated with so-called Broca's aphasia, which includes dysfluent and telegraphic speech. The medial extent of the lesion in the superior frontal gyrus is also near the SMA. Damage to the SMA is associated with "SMA syndrome," in which some patients demonstrate speech production deficits that range from diminished spontaneous speech to full mutism, despite intact comprehension (Krainik et al., 2003; Laplane, Talairach, Meininger, Bancaud, & Orgogozo, 1977). To measure verbal fluency, we used the Cookie Theft evaluation, a subtest of the Boston Diagnostic of Aphasia Examination (BDAE; Goodglass, Kaplan, & Barresi, 2001), as it is well established for measuring fluency in aphasia (Grossman et al., 2013; Sonty et al., 2003; Brookshire & Nicholas, 1994; Freedman, Alexander, & Naeser, 1984). In this test, the patient is asked to describe in 2 min everything going on in a scene presented on a piece of paper. To quantify fluency, we measured the mean length of utterance (MLU) or the average number of morphemes across each utterance produced. We analyzed MLU because it is established as a metric of verbal fluency in aphasia (e.g., Borovsky, Saygin, Bates, & Dronkers, 2007) and has been shown to correlate with damage to the FAT (Catani et al., 2013). In an additional set of exploratory analyses, we also measured the duration of every pause between words and binned the interword pauses by the grammatical class of the immediately following word. This annotation was carried out using Audacity software. Pauses were calculated by manually inspecting the end of each word and the beginning of the next word. Pauses that were less than 100 msec in duration were classified as normal pauses. Words preceded by a caugh, sneeze, yawn, and so forth, were discarded. B. C. transcribed and annotated the data, as well as two additional annotators who were blinded to participant identity and test session and naïve to variables of interest.

Picture Naming

We used picture naming (Snodgrass & Vanderwart, 1980) to test for postoperative anomia; anomia is, by definition, an impairment for accessing words from concepts and typically differentially present for nouns (Papagno et al., 2010; Hamberger, Seidel, Mckhann, Perrine, & Goodman, 2005). A subset of 80 of the original items was chosen after (Barbarotto, Laiacona, Macchi, & Capitani, 2002; see Stasenko et al., 2014).

In addition, and as noted above, each patient completed a larger battery of neuropsychological tests. The purpose of testing the patients more broadly was to understand the limits of each patient's impairments, which is critical for deriving inferences about the underling cognitive processes that are disrupted in each patient (e.g., see the "sufficiency condition" of Caramazza, 1984). The additional tests that were used were discussed below.

Category Fluency

Each patient completed a category fluency experiment in which she was asked to overtly generate as many items in 1 min as possible, from three cues: words beginning with a certain letter (e.g., "F"), words belonging to a certain category (e.g., fruits), or actions from a particular context (e.g., actions done in the kitchen).

Word Reading

The patients' ability to read visually presented words (Psycholinguistic Assessment of Language Processing in Aphasia [PALPA; Kay, Coltheart, & Lesser, 1992] subtest 33), pseudowords (PALPA subtest 36), and numbers (one, two, and three digits) was tested.

Sentence Repetition

Sentence repetition ability was evaluated using a subset of items (n = 18) from Form 1 of Subtest 12 of the PALPA. Each sentence was read to the patient by the experimenter (one at a time) and the patient was asked to immediately repeat the sentence back to the experimenter. This is a particularly relevant task to distinguish disruption of verbal fluency as predicted in the patient with a lesion adjacent to the FAT, from a general so-called Broca's aphasia—patients with Broca's aphasia are classically impaired at sentence repetition. Thus, if damage to the FAT results in disruption of speech fluency but not a general Broca's aphasia, the patient should be intact for sentence repetition.

Semantic Processing

To assess the integrity of semantic processing, apart from reading and naming ability, both patients completed multiple tests of semantic processing. In a picture–word matching task, the patients were simultaneously shown a picture and a word and indicated whether or not the picture matched the word (Stasenko et al., 2014). Patients also completed the picture version of the Pyramids and Palm Trees test (Howard & Patterson, 1992) in which they were presented with three pictures on each trial and asked to identify which of the two target pictures is more conceptually related to the cued picture. These tests are important for inferring that any difficulties that the patients have with speech production are not likely to be due to a semantic level impairment. This is particularly important for the patient who underwent a left ATL resection.

Verbal Working Memory

Working memory was evaluated using a standard digit span task where the patient is read digits and asked to immediately repeat back the digits. Both forward digit span (experimenter says 1, 5, 3 and patient responds 1, 5, 3) and backward digit span (experimenter says 1, 5, 3 and

patient responds 3, 5, 1) were assessed. Each patient's span is the maximum number of digits that can be accurately repeated (allowing three attempts at each span length).

Praxis

Both patients completed a battery to evaluate praxis. They were asked to visually identify everyday manipulable objects (e.g., toothbrush, screwdriver), demonstrate how they would use the object with their dominant hand, and explain the object's purpose. Patients AF and AG also pantomimed both transitive (e.g., show me how you would use a hammer) and intransitive (e.g., "be quiet") gestures from command and executed the same pantomimes to imitation. Last, AF and AG were shown videos of different pantomimes and asked to discriminate the meaning of the pantomime (by way of picking which object goes with the observed pantomime) and to discriminate between meaningful versus meaningless gestures (for details, see Garcea et al., 2013).

Task-based fMRI Experiments

Each patient underwent several BOLD fMRI studies designed to localize language, sensorimotor, and praxis networks as part of their pre-surgical planning; these scans constitute a standard regimen of scans conducted on all neurosurgery patients studied in our lab.

Object Recognition

Both patients completed a passive viewing experiment in which they viewed scrambled and intact images of tools, animals, famous faces, and famous places. For each of the four categories (tools, animals, faces, and places), 12 items were selected (e.g., hammer, Bill Clinton), and for each item, eight exemplars (gray-scale photographs) were selected (e.g., eight different hammers, eight different pictures of Bill Clinton). This resulted in 96 images per category and 384 total images. Phase-scrambled versions of the stimuli were created to serve as a baseline condition. Participants viewed the images in a mini-block design. Within each 6-sec mini-block, 12 stimuli from the same category were presented, each for 500 msec (0-msec ISI), and 6-sec fixation periods were presented between mini-blocks. Within each run, eight mini-blocks of intact images and four mini-blocks of phase-scrambled versions of the stimuli were presented with the constraint that a category of objects did not repeat during two successive mini-block presentations. Patients AF and AG completed eight runs of the object-responsive cortex localizer experiment (91 volumes per run; for details and precedent, see Chen, Garcea, Almeida, & Mahon, 2017; Chen, Garcea, & Mahon, 2016).

Language Mapping

Patient AF completed two language tasks preoperatively and postoperatively as part of her clinical workup before surgery (definition naming and verb generation). Patient AG completed a different language task preoperatively and postoperatively, as part of her participation in a research study (category fluency).

Patient AF: Definition Naming and Verb Generation

For verb generation, Patient AF was shown a concrete noun and was instructed to silently produce a semantically related verb (e.g., pencil–write). The experiment was organized into 30-sec blocks (10 nouns presented in block, 3 sec per trial) that alternated with "baseline" control blocks where Patient AF saw a string of "#" symbols that were approximately the same length as the nouns. The total scan time was 3 min 30 sec. For definition naming, AF viewed a short description of an object (e.g., "utensil used to cut food") and was told to covertly produce the object ("knife"). The experiment was organized into blocks of 30 sec in duration (10 trials per block, 3 sec per trial), and blocks were separated by 20 sec of fixation (a fixation cross was shown). The total scan time was 4 min 8 sec.

Patient AG: Category Fluency

In the category fluency experiment, AG viewed a cue that could be a letter (e.g., words that start with the letter "A"), a noun (e.g., fruit), or an action category (e.g., actions in sports) and had 30 sec to overtly generate as many items from that category as possible. These blocks alternated with 20-sec fixation period blocks.

Resting State fMRI

During preoperative and postoperative fMRI testing sessions, Patients AF and AG completed two runs of resting state fMRI in which they were instructed to fixate upon a white cross that was superimposed on a black screen. Each run was 180 volumes in length.

MRI Data Acquisition Parameters

Whole-brain BOLD imaging was conducted on a 3-T Siemens MAGNETOM Trio scanner with a 32-channel head coil located at the Rochester Center for Brain Imaging. High-resolution structural T1 contrast images were acquired using a magnetization prepared rapid gradient echo pulse sequence at the start of each session (repetition time [TR] = 2530 msec, echo time [TE] = 3.44 msec, flip angle = 71°, field of view [FOV] = 256 × 256 mm^2, matrix = 256 × 256, voxel size = 1 × 1 × 1 mm^3, 192 sagittal slices). Functional images were acquired using BOLD EPI pulse sequence (TR = 2000 msec, TE = 30 msec, flip angle = 90°, FOV = 256 × 256 mm^2, matrix = 64 × 64, voxel size = 4 × 4 × 4 mm^3, 30 axial slices).

Patient AF also completed scans at a different location using a 3-T GE Discovery MR750 MRI scanner (General

Electric, Milwaukee, WI) equipped with an eight-channel head coil. Functional images were acquired using BOLD EPI pulse sequence (TR = 2000 msec, TE = 30 msec, flip angle = 90°, FOV = 256 × 256 mm^2, matrix = 64 × 64, voxel size = 4 × 4 × 4 mm^3, 39 axial slices).

All DTI data were acquired at the Rochester Center for Brain Imaging, using a single-shot echo-planar sequence (60 diffusion directions with b = 1000 s/mm^2, 10 images with b = 0 s/mm^2, TR = 8900 msec, TE = 86 msec, FOV = 256 × 256 mm^2, matrix = 128 × 128, voxel size = 2 × 2 × 2 mm^3, 70 axial slices). A double-echo gradient echo field map sequence (echo time difference = 2.46 msec, EPI dwell time = 0.75 msec) was acquired with the same resolution as the DTI sequence and was used to correct for distortion caused by B0 inhomogeneity. DTI was obtained for both patients preoperatively and postoperatively using the same scanner.

Functional MRI Preprocessing

fMRI data were analyzed with the BrainVoyager software package (Version 2.8) and in-house scripts drawing on the BVQX toolbox written in MATLAB (The MathWorks, Natick, MA). The first six volumes of each run were discarded to allow for signal equilibration (four at image acquisition and two at preprocessing). Preprocessing of the functional data included, in the following order, slice scan time correction (sinc interpolation), motion correction with respect to the first volume of the first functional run, and linear trend removal in the temporal domain (cutoff: two cycles within the run). Functional data were registered (after contrast inversion of the first volume) to high-resolution de-skulled anatomy of each participant in native space. For each participant, echo-planar and anatomical volumes were transformed into standardized space (Talairach & Tournoux, 1988). We analyzed the functional data in Talairach space because they are part of a larger longitudinal study for which we compare fMRI data across patients. Although the anatomy of each patient is subject to mass effects of the lesions, the transformation to Talairach space is a linear transformation, with only rotation, translation, and scaling performed to place the brain in the AC–PC plane and fit it to the dimensions of the Talairach bounding box. Consequently, the location of a given functional voxel is determined by the Euclidean dimensions of the brain, rather than alignment of the cortical surface to a template. Functional data were smoothed at 6-mm FWHM (1.5-mm voxels) and interpolated to 3 × 3 × 3 mm^3 voxels. These analysis pipelines are also described in a prior work from our group (e.g., Chen, Garcea, Almeida, et al., 2017; Chen, Garcea, Jacobs, & Mahon, 2017; Chen et al., 2016; Garcea, Kristensen, Almeida, & Mahon, 2016; Kristensen, Garcea, Mahon, & Almeida, 2016; Garcea & Mahon, 2014; Almeida, Fintzi, & Mahon, 2013; Mahon, Kumar, & Almeida, 2013).

DTI Preprocessing

DTI preprocessing was performed with the FMRIB Software Library (FSL; www.fmrib.ox.ac.uk/fsl/). FSL's brain extraction tool (Smith, 2002) was used to skull-strip each participant's diffusion-weighted and T1 images as well as the fieldmap magnitude image. The B0 image was stripped from the diffusion-weighted image, and the fieldmap was prepared using FSL's prepare fieldmap tool. Smoothing and regularization were performed using FSL's fugue tool (www.fmrib.ox.ac.uk/fsl), and a 3-D Gaussian smoothing was applied using sigma = 4 mm. The magnitude image was then warped based on this smoothing, with y as the warp direction. Eddy current correction was performed using FSL's eddy_correct tool (Graham, Drobnjak, & Zhang, 2015), which takes each volume of the diffusion-weighted image and registers it to the B0 image to correct for both eddy currents and motion. Next, the deformed magnitude image was registered to the B0 image using FSL's linear image registration tool (Jenkinson & Smith, 2001). The resulting transformation matrix was then applied to the prepared fieldmap. Last, the diffusion-weighted image was undistorted using the registered fieldmap, with FSL's fugue tool. Intensity correction was also applied to this unwarping. Upon completion of preprocessing, FSL's DTIFIT tool was used to reconstruct the diffusion tensors. DTIFIT uses linear regression to fit a diffusion tensor model at each voxel of the preprocessed diffusion image. All tractography and microstructural measurement analyses were conducted in native diffusion space, and the data were only registered to native T1 space for visualization.

Probabilistic Tractography: FAT

Probabilistic tractography of the FAT was performed using FSL's probtrackx2 tool, which uses Bayesian estimation of the diffusion parameters (Behrens, Berg, Jbabdi, Rushworth, & Woolrich, 2007; Behrens et al., 2003). ROIs for tractography were functionally defined in each patient preoperatively, using the peak BOLD contrast from the verb generation and verbal fluency tasks, in the pre-SMA and the posterior inferior frontal gyrus. Ten-millimeter-radius spheres were drawn around the peak voxel, and 5,000 streamline samples were initiated from those spheres with a curvature threshold of 0.2 and a step length of 0.5 mm. Using the network mode option in FSL, fiber tracking was initiated from each seed ROI separately and only the streamlines that passed through the other ROI were kept.

Probabilistic Tractography: ILF

Probabilistic tractography of the ILF was also performed with probtrackx2 in FSL. ROIs were drawn as suggested by Catani and Thiebaut de Schotten (2008). Briefly, one

seed is drawn over the white matter of the occipital lobe on 13 axial slices. The second seed is drawn in the ATL on three axial slices. In addition, two exclusion masks were used. One exclusion mask was drawn around the entire frontal lobe on a single coronal slice at the edge of the genu of the corpus callosum, to avoid fibers of the inferior fronto-occipital fasciculus (Thomas et al., 2009; Wakana et al., 2007). A midline sagittal slice was also used as an exclusion mask to avoid fibers that cross into the right hemisphere. From each seed, 5,000 streamline samples were initiated, with a curvature threshold of 0.2 and a step length of 0.5 mm. Using the network mode option, fiber tracking was initiated from each seed ROI separately, unconstrained, and only the voxels that were tracked from each ROI seed going through the other ROI were kept in the resulting tractogram.

Statistical Analysis of DTI Metrics

FA, mean diffusivity (MD), RD, and axial diffusivity (AD) maps generated during tensor fitting were used to compare diffusion properties of the FAT before and after surgery. We report each of these measures—as opposed to only FA—for purposes of completeness. Analyses were carried out at several tractogram thresholds (5%, 10%, 15%, and 20% of the maximum value) to ensure that effects were robust and not due to underthresholded or overthresholded data. We also used two metrics to approximate the volume of the tract. First, we used the waytotal from each tractogram to measure the total number of streamlines. Second, we used the number of voxels in the tractogram after threshold. Each of these can be seen as an indirect measure of tract volume, which is important in the context of postoperative tractography, where portions of a tract may have been resected.

Thresholded tractograms were used to mask the whole-brain FA, MD, RD, and AD maps, and the resulting data were extracted and imported into MATLAB for analysis. Two-sample t tests were performed to compare preoperative and postoperative FA, MD, RD, and AD values. F tests for equal variance showed that, across each metric and each threshold, variance was unequal in the distribution of preoperative and postoperative tracts ($ps < .001$, all thresholds and metrics). Accordingly, all t tests used were performed with Satterthwaite's approximations to compensate for unequal variance.

Functional Connectivity

All functional connectivity analyses were time course based using the time series from the entire run. The change in head position across volumes was regressed out of the time series data, after preprocessing steps described above. All functional connectivity analyses were conducted over the residuals of that regression model. We did not regress the global mean time course, as recent work has suggested that this procedure is at best unnecessary and, at worst, may introduce spurious patterns to the data (e.g., see Gotts et al., 2013). Whole-brain functional connectivity maps were restricted with a mask fit to the average de-skulled Talairached anatomy. Note that the core contribution of the functional connectivity analyses is to test for convergence with the DTI data and specifically for a double dissociation across the two patients.

Functional connectivity was measured between ROIs defined functionally using the verb generation and verbal fluency experiments, as described above. Functional definition of the ROIs minimizes a possible bias that can come with manual delineation based on anatomical landmarks. We did not define ROIs based on automatic parcellation of anatomical regions or atlases to minimize the complications introduced by mass effect caused by the tumors. Critically, the definition of ROIs and the measurement of functional connectivity were done separately and with independent data sets, to avoid circularity. Functional connectivity between two regions was measured by correlating the time course of BOLD signal averaged across all voxels in one ROI with the time course of BOLD signal averaged across all voxels in the other ROI. We measured functional connectivity between two pairs of regions, the posterior inferior frontal gyrus and pre-SMA as well as the posterior inferior frontal gyrus and the middle temporal gyrus.

It should also be noted that, although we measured functional connectivity between the posterior inferior frontal gyrus and the middle temporal gyrus, the ILF does not directly connect these two cortical regions. However, we chose to measure between these ROIs for two reasons. First, we defined our ROIs functionally and were careful to avoid testing functional connectivity in regions of the brain that were resected, which includes much of the anterior inferior temporal lobe for Patient AG. Second, we were interested in a double dissociation between areas of the brain connected to the inferior frontal gyrus. The inferior frontal gyrus is connected to the ATL via the uncinate fasciculus (Leng et al., 2016; Jellison et al., 2004), and the inferior frontal gyrus is connected to the deep middle temporal gyrus via the inferior fronto-occipital fasciculus. The ATL is connected to posterior temporal and occipital areas via the ILF. Third, although recent work has found a relation between damage to the ILF and anomia (Herbet et al., 2016), some intraoperative evidence indicates that stimulation of the ILF does not disrupt picture naming, perhaps because the role of the inferior fronto-occipital fasciculus may be sufficient and, potentially to some degree, redundant in supporting naming (Mandonnet, Nouet, Gatignol, Capelle, & Duffau, 2007).

All functional connectivity analyses were carried out both preoperatively and postoperatively on all available functional runs except for runs used to define ROIs, including passive viewing of objects (tools, animals, faces, and places), a category fluency experiment, verb generation,

definition naming, and resting state scans. Functional connectivity was computed at the run level, and Fisher-transformed correlation values were then compared using *t* tests to assess possible changes in functional connectivity as a function of surgery.

RESULTS

Neuropsychological Testing

After surgery, neither patient (AF nor AG) exhibited impairments of voluntary manual movements, praxis, semantic processing, language comprehension, or sentence repetition (see Table 1). Limb movements were smooth, continuous, and efficient, with no observable hesitation or jerking in either patient. Neither patient had difficulty with movement in day-to-day life. However, the two patients exhibited dissociable speech production deficits. Patient AF, whose surgery partially resected the FAT, exhibited difficulty with producing fluent sentences but was not impaired at picture naming, whereas Patient AG was impaired at picture naming and exhibited a moderate anomia but had no other difficulties with spontaneous speech. Neither patient produced semantic or phonemic paraphasias. Importantly, neither patient was impaired for reading words or pseudowords. The lack of impairment for voluntary movements is important for ruling out a general deficit for motor initiation in Patient AF and indicates that her difficulties with initiating spontaneous speech are not general to any voluntary motor task. It is also worth underlining that Patient AF was not impaired for repeating sentences, thus ruling out a general impairment with speech production (i.e., a so-called "Broca's aphasia"). Similarly, the fact that neither patient was impaired for reading words or pseudowords indicates that their respective language difficulties were not at the level of phonological encoding or articulatory processes; the fact that neither patient exhibited visual or semantic impairments indicates that the difficulties with speech production are not attributable to semantic confusion (in the case of AF) or difficulty processing pictures (in the case of AG).

We quantified the difficulties that Patient AF exhibited with verbal fluency by measuring the MLU; postoperatively, there was a reduction in MLU in Patient AF, but not in Patient AG (Figure 1A). We also analyzed where pauses occurred in spontaneous speech (Cookie Theft picture description test); Patient AF paused more frequently before verbs and verb phrases. Of 11 pauses between utterances, nine came before the subject of a verb phrase ($n = 5$) or the verb itself ($n = 4$; two additional pauses before an adjective and an adverb). The mean duration of pauses was 12.16 sec before the subject of a verb phrase ($SD = 5.76$ sec), 3.21 sec before the verb itself ($SD = 1.44$ sec), and 3.05 sec for the other two pauses ($SD = 1.43$ sec). By comparison, Patient AG produced more speech with more frequent but much shorter pauses. Fifteen of 29 pauses came before a noun ($n = 11$) or noun phrase ($n = 4$). Only five pauses came before a verb ($n = 2$) or verb phrase ($n = 3$). An additional five pauses came before a preposition; two, before a conjunction; and two, before an adjective. The mean duration of pauses was 1.09 sec before a noun ($SD = 1.7$ sec), 0.47 sec before the head of a noun phrase ($SD = 0.26$ sec), 0.33 sec before a verb ($SD = 0.01$ sec), and 0.57 sec before the subject of a verb phrase ($SD = 0.56$ sec). The mean duration for the pauses was 0.21 sec before a preposition ($SD = 0.05$ sec), 0.48 sec before a conjunction ($SD = 0.35$ sec), and 0.55 sec before an adjective ($SD = 0.33$ sec).

The opposite dissociation across the two patients was observed when looking at picture naming performance: Patient AF's accuracy was slightly better postoperatively, with no change in RT (see Figure 1B). By comparison, Patient AG's accuracy decreased from 95% preoperatively to 74% postoperatively ($t(158) = 4.36$, $p < .001$, $d = 0.49$), and her correct trials were slower postoperatively than preoperatively ($t(158) = 5.40$, $p < .001$, $d = 0.96$).

Probabilistic Tractography: Patient AF (Frontal Lobe Surgery)

Probabilistic tractography successfully reconstructed the FAT in both the left and right hemispheres, preoperatively and postoperatively, as well as the left ILF (see Figure 2). The waytotal for the preoperative left hemisphere FAT was 623,757. Postoperatively, the left-hemisphere FAT waytotal decreased to 40,957 (a 93% decrease). The number of voxels contained within the tract decreased by an average of 148 voxels (range = 96–253 voxels) across all thresholds, an average decrease of 32.3%. Despite contiguous bundles of the FAT successfully reconstructed both before and after surgery, clear changes in the diffusivity measures were observed after surgery. Of note, FA decreased after surgery (see Figure 3). This effect was robust across thresholds (see Tables 2 and 3). MD, RD, and AD significantly increased across all thresholds. By comparison, there was no change in FA postoperatively in the ILF in Patient AF (see Figure 1). Additional analyses (not reported herein) in which we adjusted the sizes of the spheres used as seeds for the DTI analysis (decreased and increased by 2 and 4 mm) did not change any of these core findings. Those control analyses indicated that the decision to use 1-cm sphere for fiber tracking did not affect the overall pattern of the findings.

Probabilistic Tractography: Patient AG (ATL Surgery)

The left and right FAT and the left ILF were tracked in Patient AG preoperatively and postoperatively. For the FAT, there were no significant changes in FA, MD, or RD, or AD postoperatively, regardless of threshold (see Tables 2 and 3). For the ILF, we found that the waytotal

Table 1. Full Neuropsychological Performance of Each Patient Preoperatively and Postoperatively

Test	*Patient AF Preop*	*Patient AF Postop*	*Patient AG Preop*	*Patient AG Postop*
Date	*3/16/12*	*See Below*	*4/12/16*	*6/29/16*
Verbal fluency: letter	-	3[2] | 9.66[3]	16.1	9.8
Verbal fluency: nouns	-	9.5[2] | 9.5[3]	14.7	9.3
Verbal fluency: actions	-	8.2[3]	14.4	10.4
Cookie Theft	17.8	6[1] | 6.8[2] |8.5[3]	10.8	11.4
Pyramids & Palmtrees	89	85.4[2] | 96.36[3]	-	89
Kissing and dancing	94	57.7[1] | 98.1[3]	85	100
Object decision	92.5	85.6[1] | 91.25[2]	100	97.5
Picture–word matching	95	62.5[1] | 95.8[2]	100	93
Digit span forward	8	8[1] | 8[3]	5	6
Digit span backward	3	3[1] | 3[3]	4	5
Sentence repetition	100	100[1] | 100[2] |100[3]	100	94.4
Snodgrass long	95.7	95.7[1] | 98[3]	95	73.75
Word reading: GramClass	100	100[1]	-	-
Word reading: GramClassXImage	100	95[1] | 100[3]	95	95
Word reading: ImageXFreq	100	98.75[1]	-	-
Word reading: Regularity	100	100[1]	-	-
Pseudoword reading	100	100[1]	100	91.7
Number naming	100	-	100	100
Pantomime discrimination	88.9	77.8[1]	100	100
Action discrimination	100	100[1]	88.9	83.3
Action imitation: transitive	100	100[1] | 92[2]	100	100
Action imitation: intransitive	100	100[1] | 100[2]	100	100
Bag of tools: ID	100	93[2]	100	83
Bag of tools: pantomime	100	93[2]	100	100
Bag of tools: function	100	93[2]	100	100
Point light walker	100	100[1]	100	100
Arithmetic	-	-	87.5	87.5
Cambridge face test	-	-	75	80
Object function	-	-	95.8	91.7
Object manipulation	-	-	39	39
Neglect (bells + line bisection)	-	-	100	100
Semantic attribution questionnaire	-	-	-	95.8

Values in the table represent percent accuracy, with the exception of digit span (number of digits), Cookie Theft (MLU), and verbal fluency (mean number of items).

[1]Date: April 27, 2012. [2]Date: June 14, 2012. [3]Date: February 20, 2015.

decreased from 2,228,770 preoperatively to 894,166 (a 60% decrease). The number of voxels contained within the tract decreased by an average of 482 voxels (range = 189–931 voxels) across all thresholds, an average decrease of 35.4%. Mean FA and AD both increased postoperatively. It is known that, along the ILF, anterior portions have significantly lower FA values, even in healthy individuals (Galantucci et al., 2011). Thus, resection of the anterior

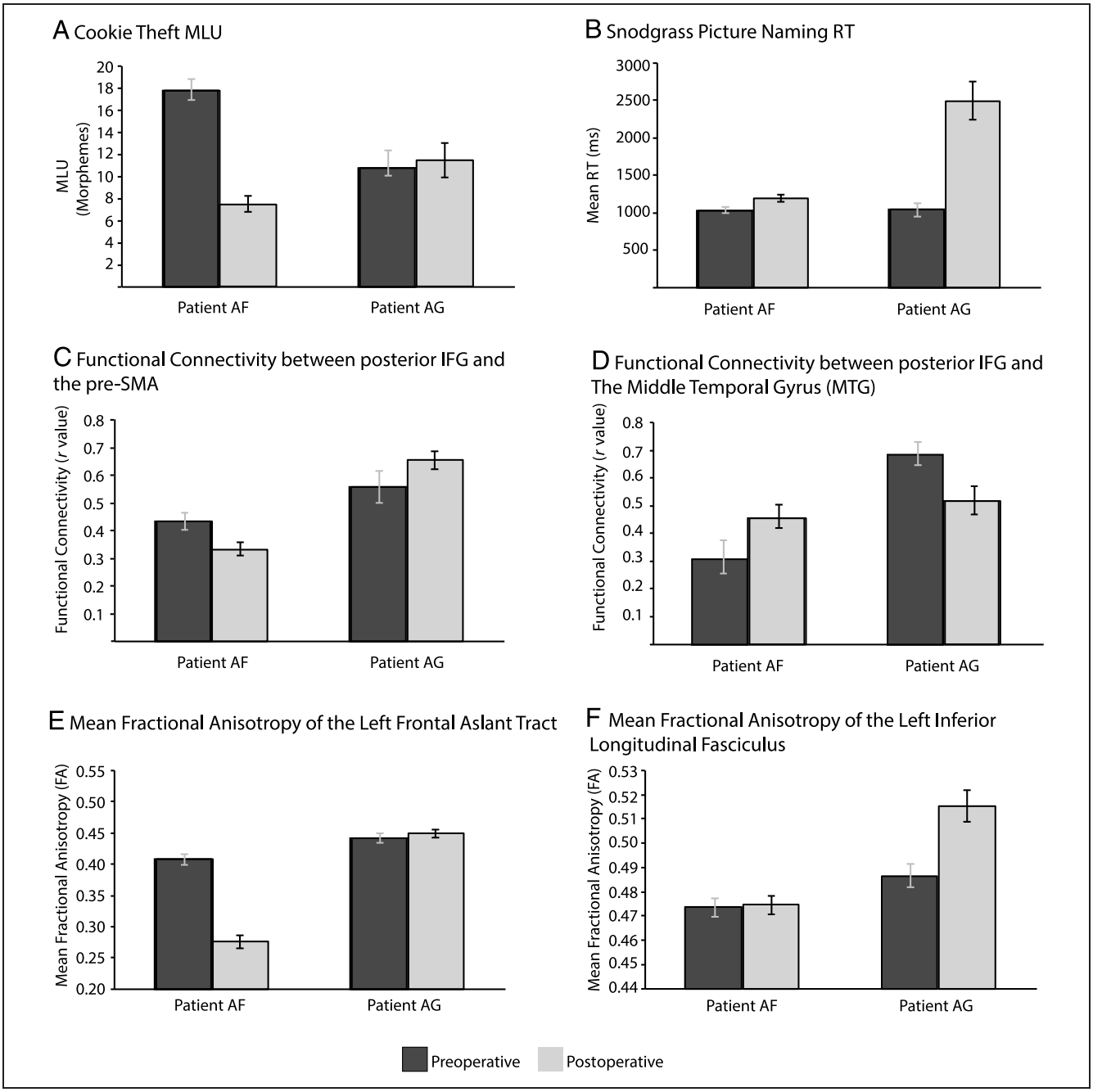

Figure 1. Preoperative and postoperative behavioral and MRI findings. (A) MLU in the Cookie Theft test of spontaneous speech. Patient AF completed the test multiple times postoperatively (see Table 1), with the average MLU shown plotted in A. (B) Mean RT of each patient, preoperatively and postoperatively, averaged over 80 trials of picture naming. (C) Mean functional connectivity between the posterior inferior frontal gyrus (IFG) and the pre-SMA over all BOLD scans (excluding scans used to functionally define language areas) for each patient, preoperatively and postoperatively. (D) Mean functional connectivity between the posterior IFG and the middle temporal gyrus over all BOLD scans for each patient, preoperatively and postoperatively. (E) Mean FA of the left FAT for each patient, preoperatively and postoperatively. Averages plotted here were calculated at the 15% threshold (see Table 2 for other thresholds). Error bars show the standard error of the mean, over voxels. (F) Mean FA of the left ILF for each patient, preoperatively and postoperatively. Averages were calculated at the 15% threshold. Error bars show the standard error of the mean, over voxels.

portion of the ILF could, in principle, be responsible for the overall increase in FA (because voxels that typically represent the lower distribution of FA values for that tract were resected). Again, there were no changes to the core effects when the sizes of the spheres used as seeds in the DTI analyses was increased or decreased by up to 4 mm.

Functional Connectivity

We observed a double dissociation across the two patients: Functional connectivity between the pre-SMA and the posterior inferior frontal gyrus decreased for Patient AF as a function of surgery but was unchanged

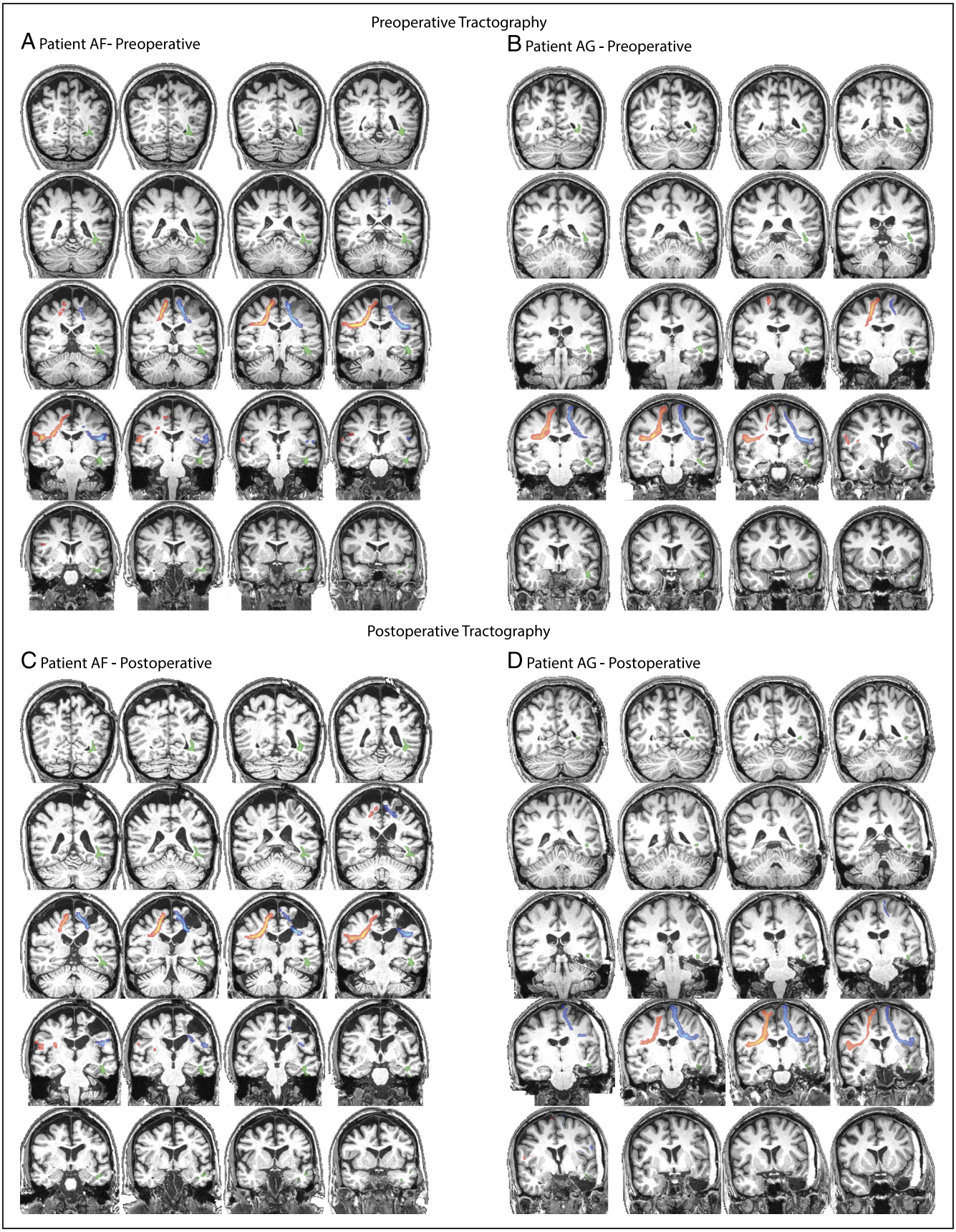

Figure 2. Preoperative and postoperative tractography of the left and right FATs and the left ILF. Tracts are shown at the 15% threshold and are warped into each participant's native anatomical (T1-weighted) space. Each tractogram is visualized as a heat map representing relative probability. Red/yellow: right FAT. Blue/light blue: left FAT. Green/light green: left ILF.

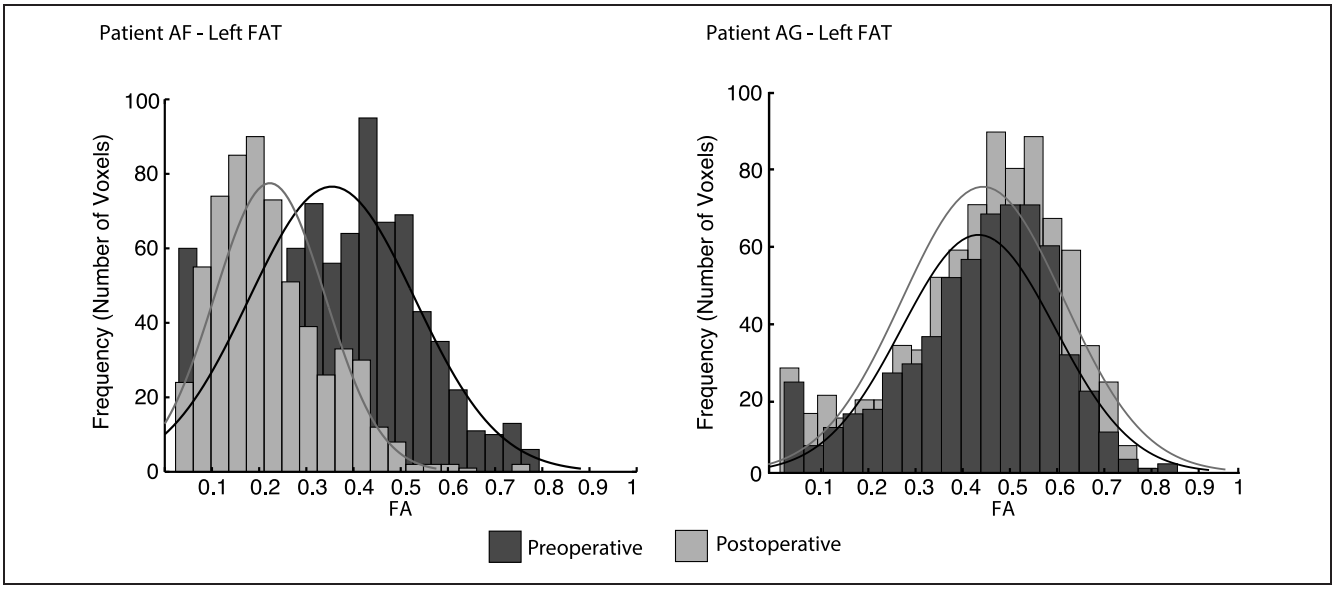

Figure 3. Voxelwise distribution of the preoperative and postoperative left FAT for each patient. Distributions shown here were calculated at the 15% threshold.

for Patient AG. In contrast, functional connectivity between the middle temporal gyrus and inferior frontal gyrus decreased for Patient AG but was unchanged for Patient AF (see Figure 1). The three-way ANOVA with factors Patient (two levels: patient AF, patient AG), ROI pairs (two levels: the posterior inferior frontal gyrus and the middle temporal gyrus, the posterior inferior frontal gyrus and the pre-SMA), and Test session (two levels: preoperative, postoperative) was significant ($F(1, 81) = 15.66, p < .001, \eta_p^2 = 0.20$). The two-way interactions were not significant between Patient and ROI ($F < 1$), Patient and Test session ($F < 1$), or ROI and Test session ($F < 1$). However, within each patient, there were significant two-way interactions between ROI and Test session (AF: $F(1, 47) = 9.44, p < .005, \eta_p^2 = 0.18$; AG: $F(1, 23) = 6.47, p < .02, \eta_p^2 = 0.24$). The only significant main effect was that of Patient ($F(1,81) = 36.4, p < .001, \eta_p^2 = 0.40$). Hypothesis-driven tests for each pair of ROIs for each patient indicated that the reduction between test sessions in functional connectivity supported by the Frontal Aslant Tract was significant for AF ($t(23) = 2.60, p < .02, d = 1.06$) but not for AG ($t(11) = -1.43, p = .178, d = 0.67$); in contrast, the reduction in functional connectivity supported (in part) by the inferior longitudinal fasciculus was significant for AG ($t(11) = 2.54, p = < .03, d = 1.20$) but not for AF ($t(23) = -2.02, p = .06, d = 0.82$).

DISCUSSION

We have reported a double dissociation in language abilities across two neurosurgical case studies that were evaluated for language ability preoperatively and postoperatively. Patient AF, who underwent surgery to remove a left frontal glioma, exhibited a postoperative speech production impairment with little or no impairment to lexical access (picture naming remained at preoperative level). Patient AG, who underwent resection of the left ATL to access and remove a left hippocampal tumor, exhibited a moderate impairment for producing nouns but no other difficulties with spontaneous speech. Neither patient had difficulties postoperatively with word reading, nonverbal tests of semantic processing, praxis, or motor function. Both DTI and functional connectivity analyses indicated that, in Patient AF, there was a disconnection between the left inferior frontal gyrus and the pre-SMA, but no change in the ILF. In contrast, in Patient AG, there was a reduction of connectivity supported by the ILF but no change in connectivity supported by the FAT. Although interpretation of diffusion metrics such as FA, RD, and AD remains a matter of discussion (Paul et al., 2014; Tournier, Mori, & Leemans, 2011; Beaulieu, 2002; Song et al., 2002), the contribution of the DTI data in this context does not depend on the putative neurobiological basis of the diffusion indices but rather on the pattern of dissociation across the two patients and alignment to other measures (functional connectivity, behavior) that also dissociate across the two patients.

Patient AF's difficulties with spontaneous speech converge with prior evidence implicating the pre-SMA in speech production, including studies conducted with healthy individuals (Alario, Chainay, Lehericy, & Cohen, 2006) and in lesion studies (Vergani et al., 2014). Speech production impairments in patients with pre-SMA lesions have been described as transcortical motor aphasia, a nonfluent aphasia distinct from classical Broca's aphasia in that sentence repetition is intact. Critically, Patient AF did not have trouble repeating sentences either preoperatively or postoperatively. In addition, although there is emerging evidence suggesting that the FAT may be important for nonspeech or motor/supramotor

Table 2. Microstructural Properties of the Left Preoperative and Postoperative FAT

Patient AF: Left FAT				
Threshold	*Preop Mean FA (SD)*	*Postop Mean FA (SD)*	*t Stat*	*p*
5	0.36 (0.18)	0.27 (0.17)	9.68	1.61E-21
10	0.39 (0.16)	0.28 (0.16)	9.5	2.59E-20
15	0.41 (0.16)	0.28 (0.16)	9.46	1.72E-19
20	0.41 (0.15)	0.25 (0.12)	11.25	2.69E-25
Threshold	*Preop Mean MD (SD)*	*Postop Mean MD (SD)*	*t Stat*	*p*
5	0.86 (0.40)	1.19 (0.46)	−14.64	5.96E-45
10	0.78 (0.18)	1.15 (0.38)	−16.65	2.77E-49
15	0.77 (0.14)	1.17 (0.36)	−15.33	4.69E-38
20	0.76 (0.12)	1.22 (0.34)	−15.54	3.49E-34
Threshold	*Preop Mean RD (SD)*	*Postop Mean RD (SD)*	*t Stat*	*p*
5	0.71 (0.42)	1.04 (0.49)	−13.55	4.01E-39
10	0.62 (0.22)	0.99 (0.41)	−15.25	2.12E-43
15	0.60 (0.18)	1.01 (0.39)	−14.28	7.76E-35
20	0.59 (0.16)	1.07 (0.36)	−15.18	6.30E-34
Threshold	*Preop Mean AD (SD)*	*Postop Mean AD (SD)*	*t Stat*	*p*
5	1.17 (0.38)	1.50 (0.45)	−15.15	1.15E-47
10	1.12 (0.19)	1.48 (0.39)	−15.91	5.49E-46
15	1.12 (0.17)	1.50 (0.37)	−13.88	1.88E-33
20	1.11 (0.16)	1.54 (0.35)	−13.72	7.10E-30
Patient AG: Left FAT				
Threshold	*Preop Mean FA (SD)*	*Postop Mean FA (SD)*	*t Stat*	*p*
5	0.40 (0.16)	0.40 (0.18)	−0.78	.44
10	0.42 (0.15)	0.43 (0.16)	−0.98	.33
15	0.44 (0.14)	0.45 (0.16)	−0.80	.42
20	0.45 (0.14)	0.46 (0.15)	−0.91	.36
Threshold	*Preop Mean MD (SD)*	*Postop Mean MD (SD)*	*t Stat*	*p*
5	0.80 (0.31)	0.79 (0.31)	0.28	.78
10	0.77 (0.27)	0.76 (0.26)	0.57	.57
15	0.73 (0.15)	0.74 (0.22)	−1.49	.14
20	0.71 (0.09)	0.74 (0.19)	−2.17	.03

Table 2. (*continued*)

Patient AF: Left FAT				
Threshold	*Preop Mean FA (SD)*	*Postop Mean FA (SD)*	*t Stat*	*p*
5	0.63 (0.34)	0.63 (0.35)	0.28	.78
10	0.59 (0.30)	0.58 (0.30)	0.60	.55
15	0.54 (0.17)	0.56 (0.25)	−1.02	.31
20	0.53 (0.12)	0.54 (0.22)	−1.31	.19
Threshold	*Preop Mean AD (SD)*	*Postop Mean AD (SD)*	*t Stat*	*p*
5	1.13 (0.29)	1.13 (0.28)	0.23	.82
10	1.12 (0.26)	1.12 (0.25)	0.35	.73
15	1.09 (0.19)	1.12 (0.22)	−1.85	.06
20	1.08 (0.16)	1.12 (0.20)	−2.62	.01

Two-sample *t* tests between preoperative and postoperative distributions are calculated at each threshold for each metric. Correction for unequal variance was applied to estimate the proper degrees of freedom. MD, RD, and AD values are scaled by a factor of 10^3.

processes including reaching and grasping (Budisavljevic et al., 2017), neither of the patients reported here exhibited any difficulty with nonspeech motor functions. It is also important to note that Patient AF did not exhibit motor-speech-related deficits; rather, her difficulties seem to relate more to planning multiword utterances.

Situating the FAT in models of speech production is an important step in understanding its functional role. Evidence from direct electrical stimulation in awake neurosurgery patients has contributed to a hodotopic model of language processing proposed by Duffau and colleagues (Duffau, Moritz-Gasser, & Mandonnet, 2014; Duffau, Herbet, & Moritz-Gasser, 2013). In that model, the FAT is proposed to operate in parallel with a ventral semantic system (ILF, inferior frontal occipital fasciculus, uncinate) and a dorsal phonological system (arcuate fasciculus, superior longitudinal fasciculus) in support of speech production. Although successful language processing relies on functional interactions between the posterior inferior frontal gyrus and regions in both systems, damage to the structural connections of one system (but not the other) may explain the type of dissociable language impairments described here (see also Hickok & Poeppel, 2000, 2007).

Another neurocognitive framework for language processing is the Directions Into Velocities of Articulators (DIVA) model (Guenther, 1995), which proposes both a feed-forward control system and a feedback control system whereby the neural representations of speech sounds are represented in sets of cells known as "maps." Successful control of the vocal tract involves the integration of several different maps, each of which is controlled by a network of brain regions. In that model, the pre-SMA and the left inferior frontal gyrus both provide feed-forward information: The pre-SMA is important for the model's initiation map, whereas the inferior frontal gyrus is important for the model's speech sound map (Tourville & Guenther, 2011). There is neuroimaging (Tremblay & Small, 2011; Peeva et al., 2010; Tremblay & Gracco, 2010) and TMS (Tremblay & Gracco, 2009) evidence to support a role of the pre-SMA in phonemic processing and response selection. The gradient order DIVA (GODIVA) model has extended the DIVA model and postulates that the pre-SMA may contain information about abstract structural frames, whereas the more posterior SMA contributes more to the actual initiation of the already planned speech sounds (Bohland, Bullock, & Guenther, 2010). Although it is clear that regions in the GODIVA network work together for successful speech production, more research is needed to test how damage to white matter pathways connecting those regions manifests as dissociable speech productions deficits. This converges with the pilot analyses reported above that found differentially longer pauses before verbs and verb phrases in the patient with damage to the FAT. Nonetheless, these suggestions must be regarded as speculative, and future planned research guided by these theoretical frameworks is necessary to advance understanding of the role played by the FAT in the DIVA and GODIVA models. Additional future work will also seek a more robust integration of neurobiological models of language function with cognitive and computational models of speech production (e.g., see recent discussion in Anders, Riès, Van Maanen, & Alario, 2017; Belke, 2017; Oppenheim, 2017; Schnur, 2017).

Limitations of the Current Investigation

There are two important limitations that attend the current investigation and interact with the core conclusions as articulated above. Perhaps, the most substantive of those concerns is that it cannot be known on the basis

Table 3. Microstructural Properties of the Right Preoperative and Postoperative FAT

Patient AF: Right FAT				
Threshold	*Preop Mean FA (SD)*	*Postop Mean FA (SD)*	*t Stat*	*p*
5	0.34 (0.17)	0.32 (0.15)	2.01	.04
10	0.37 (0.15)	0.36 (0.13)	1.59	.11
15	0.40 (0.14)	0.38 (0.12)	2.29	.02
20	0.41 (0.14)	0.39 (0.11)	1.57	.12
Threshold	*Preop Mean MD (SD)*	*Postop Mean MD (SD)*	*t Stat*	*p*
5	0.90 (0.49)	0.89 (0.40)	0.42	.68
10	0.79 (0.28)	0.80 (0.22)	−0.64	.52
15	0.75 (0.21)	0.77 (0.14)	−2.07	.04
20	0.73 (0.15)	0.77 (0.10)	−3.27	.001
Threshold	*Preop Mean RD (SD)*	*Postop Mean RD (SD)*	*t Stat*	*p*
5	0.76 (0.52)	0.75 (0.43)	0.28	.78
10	0.63 (0.31)	0.64 (0.24)	−0.65	.51
15	0.58 (0.23)	0.61 (0.15)	−2.24	.03
20	0.56 (0.16)	0.60 (0.11)	−3.15	.002
Threshold	*Preop Mean AD (SD)*	*Postop Mean AD (SD)*	*t Stat*	*p*
5	1.18 (0.47)	1.16 (0.38)	0.70	.48
10	1.10 (0.29)	1.11 (0.24)	−0.47	.64
15	1.08 (0.24)	1.10 (0.20)	−1.06	.29
20	1.07 (0.21)	1.10 (0.19)	−1.87	.06
Patient AG: Right FAT				
Threshold	*Preop Mean FA (SD)*	*Postop Mean FA (SD)*	*t Stat*	*p*
5	0.37 (0.17)	0.39 (0.17)	−1.63	.09
10	0.41 (0.15)	0.42 (0.15)	−1.12	.03
15	0.43 (0.13)	0.44 (0.14)	−0.67	.50
20	0.44 (0.12)	0.44 (0.14)	0.37	.71
Threshold	*Preop Mean MD (SD)*	*Postop Mean MD (SD)*	*t Stat*	*p*
5	0.83 (0.35)	0.81 (0.36)	0.98	.33
10	0.76 (0.22)	0.76 (0.25)	0.05	.96
15	0.73 (0.14)	0.74 (0.20)	−0.68	.50
20	0.72 (0.09)	0.74 (0.20)	−1.69	.092

Table 3. (*continued*)

Patient AF: Right FAT				
Threshold	*Preop Mean FA (SD)*	*Postop Mean FA (SD)*	*t Stat*	*p*
5	0.67 (0.39)	0.65 (0.40)	1.26	.21
10	0.59 (0.25)	0.59 (0.29)	0.53	.59
15	0.56 (0.17)	0.56 (0.23)	−0.43	.67
20	0.54 (0.12)	0.56 (0.23)	−1.56	.12
Threshold	*Preop Mean AD (SD)*	*Postop Mean AD (SD)*	*t Stat*	*p*
5	1.14 (0.31)	1.14 (0.32)	0.13	.90
10	1.10 (0.22)	1.11 (0.24)	−1.11	.27
15	1.08 (0.17)	1.10 (0.20)	−0.97	.33
20	1.08 (0.15)	1.10 (0.20)	−1.26	.21

Two-sample *t* tests between preoperative and postoperative distributions are calculated at each threshold for each metric. Correction for unequal variance was applied to estimate the proper degrees of freedom. MD, RD, and AD values are scaled by a factor of 10^3.

of the current study alone whether the pattern of impaired verbal fluency in Patient AF is due to the degraded structural connection between the posterior inferior frontal gyrus and the pre-SMA or whether the resection of gray matter in the frontal lobe is responsible for the observed deficit. One argument against a possible cortical role in Patient AF's postoperative language impairment is provided by the fact that intraoperative awake cortical mapping was used for both patients to avoid resection of eloquent cortical tissue. During surgery, both patients performed a picture-naming task while the surgeon stimulated the brain (neither patient underwent subcortical stimulation during tumor resection). For both patients, the surgeons respected the boundaries (within 1 cm in the same gyrus) of stimulation-induced errors during the intraoperative picture-naming task; this fact reduces the likelihood that AF's postoperative language difficulties resulted from the cortical resection associated with the surgery. We thus suggest that, given what is known about the role of the FAT in speech production, the most likely interpretation is that AF's postoperative language difficulties were due to the (partial) transection of that white matter pathway.

A second limitation associated with our conclusion has to do with why AF did not recover in the short period that is typical of patients with so-called SMA syndrome. In addition to the FAT, other white matter pathways were likely impacted by the surgery, in particular, short U-shaped fibers that connect the superior frontal gyrus to the middle frontal gyrus as well as fibers that connect the middle frontal gyrus to the inferior frontal gyrus (Catani et al., 2012). There are also callosal fibers connecting the left and right SMA that may have been affected by this resection. Thus, in Patient AF, there may have been a "triple disconnection,"[1] whereby all three of these pathways—FAT, U-shaped fibers, and callosal fibers—were impacted by the surgery. That "triple disconnection" could potentially explain the prolonged deficit in verbal fluency observed in Patient AF. This interpretation must remain speculative on the basis of the current study.

Conclusion

Speech requires retrieving a word from the mental lexicon in advance of when it will need to be uttered. Thus, the system must have some way of knowing which words will be available for a given syntactic frame, in advance of articulation. We suggest that one possible implication of our findings is that the left FAT may be critical for this component of speech production—specifically, the FAT may mediate interactions between sentence planning (construction of a syntactic frame, driven for instance by a main verb) and lexical access. This interpretation is preliminarily supported by the observation that the pauses in Patient AF's speech were more prevalent and longer before the initiation of a verb phrase whereas pauses in Patient AG's speech were more prevalent and were longer before nouns. Future studies of patients with focal lesions that combine detailed assessment of language function with functional and structural MRI would provide key causal evidence about the specific computations that are supported by the FAT.

Acknowledgments

This work was supported by NIH grants R21NS076176 and R01NS089609 and NSF grant 1349042 to B. Z. M., contributions by Norman and Arlene Leenhouts to the Department of Neurosurgery at the University of Rochester, and a core grant to the Center for Visual Science (P30 EY001319). B. L. C. was supported

by an NSF training grant (NSF DGE-1449828); F. E. G. was supported by a University of Rochester Center for Visual Science predoctoral training fellowship (5T32EY007125-24). We thank Sarah Gannon and Steve Erickson for their technical assistance in the operating room.

Reprint requests should be sent to Bradford Z. Mahon, Meliora Hall, University of Rochester, Rochester, NY 14627-0268, or via e-mail: mahon@rcbi.rochester.edu.

Note

1. We are grateful to Dr. Marco Catani, personal communication, for pointing out the possible contribution to the neuropsychological profile of this patient by this "triple disconnection."

REFERENCES

Alario, F. X., Chainay, H., Lehericy, S., & Cohen, L. (2006). The role of the motor area (SMA) in word production. *Brain Research, 1076,* 129–143.

Almeida, J., Fintzi, A. R., & Mahon, B. Z. (2013). Tool manipulation knowledge is retrieved by way of the ventral visual object processing pathway. *Cortex, 49,* 2334–2344.

Anders, R., Riès, S., Van Maanen, L., & Alario, F. X. (2017). Lesions to the left lateral prefrontal cortex impair decision threshold adjustment for lexical selection. *Cognitive Neuropsychology, 34,* 1–20.

Barbarotto, R., Laiacona, M., Macchi, V., & Capitani, E. (2002). Picture reality decision, semantic categories and gender: A new set of pictures, with norms and an experimental study. *Neuropsychologia, 40,* 1637–1653.

Beaulieu, C. (2002). The basis of anisotropic water diffusion in the nervous system—A technical review. *NMR in Biomedicine, 15,* 435–455.

Behrens, T. E. J., Berg, H. J., Jbabdi, S., Rushworth, M. F. S., & Woolrich, M. W. (2007). Probabilistic diffusion tractography with multiple fibre orientations: What can we gain? *Neuroimage, 34,* 144–155.

Behrens, T. E. J., Woolrich, M. W., Jenkinson, M., Johansen-Berg, H., Nunes, R. G., Clare, S., et al. (2003). Characterization and propagation of uncertainty in diffusion-weighted MR imaging. *Magnetic Resonance in Medicine, 50,* 1077–1088.

Belke, E. (2017). Effects of lesions to the left lateral prefrontal cortex on task-specific top-down biases and response strategies in blocked-cyclic naming. *Cognitive Neuropsychology, 34,* 26–32.

Bohland, J. W., Bullock, D., & Guenther, F. H. (2010). Neural representations and mechanisms for the performance of simple speech sequences. *Journal of Cognitive Neuroscience, 22,* 1504–1529.

Borovsky, A., Saygin, A. P., Bates, E., & Dronkers, N. (2007). Lesion correlates of conversational speech production deficits. *Neuropsychologia, 45,* 2525–2533.

Brookshire, R. H., & Nicholas, L. E. (1994). Test–retest stability of measures of connected speech in aphasia. *Clinical Aphasiology, 22,* 119–133.

Budisavljevic, S., Dell'Acqua, F., Djordjilovic, V., Miotto, D., Motta, R., & Castiello, U. (2017). The role of the frontal aslant tract and premotor connections in visually guided hand movements. *Neuroimage, 146,* 419–428.

Cai, S., Tourville, J. A., Beal, D. S., Perkell, J. S., Guenther, F. H., & Ghosh, S. S. (2014). Diffusion imaging of cerebral white matter in persons who stutter: Evidence for network-level anomalies. *Frontiers in Human Neuroscience, 8,* 54.

Caramazza, A. (1984). The logic of neuropsychological research and the problem of patient classification in aphasia. *Brain and Language, 21,* 9–20.

Catani, M., Dell'Acqua, F., Vergani, F., Malik, F., Hodge, H., Roy, P., et al. (2012). Short frontal lobe connections of the human brain. *Cortex, 48,* 273–291.

Catani, M., Howard, R. J., Pajevic, S., & Jones, D. K. (2002). Virtual in vivo interactive dissection of white matter fasciculi in the human brain. *Neuroimage, 17,* 77–94.

Catani, M., Mesulam, M. M., Jakobsen, E., Malik, F., Martersteck, A., Wieneke, C., et al. (2013). A novel frontal pathway underlies verbal fluency in primary progressive aphasia. *Brain, 136,* 2619–2628.

Catani, M., & Thiebaut de Schotten, M. (2008). A diffusion tensor imaging tractography atlas for virtual in vivo dissections. *Cortex, 44,* 1105–1132.

Chang, S. E., Erickson, K. I., Ambrose, N. G., Hasegawa-Johnson, M. A., & Ludlow, C. L. (2008). Brain anatomy differences in childhood stuttering. *Neuroimage, 39,* 1333–1344.

Chen, Q., Garcea, F. E., Almeida, J., & Mahon, B. Z. (2017). Connectivity-based constraints on category-specificity in the ventral object processing pathway. *Neuropsychologia, 105,* 184–196.

Chen, Q., Garcea, F. E., Jacobs, R. A., & Mahon, B. Z. (2017). Abstract representations of object-directed action in the left inferior parietal lobule. *Cerebral Cortex*. doi: 10.1093/cercor/bhx120.

Chen, Q., Garcea, F. E., & Mahon, B. Z. (2016). The representation of object-directed action and function knowledge in the human brain. *Cerebral Cortex, 26,* 1609–1618.

Dick, A. S., Bernal, B., & Tremblay, P. (2014). The language connectome new pathways, new concepts. *The Neuroscientist, 20,* 453–467.

Duffau, H., Herbet, G., & Moritz-Gasser, S. (2013). Toward a pluri-component, multimodal, and dynamic organization of the ventral semantic stream in humans: Lessons from stimulation mapping in awake patients. *Frontiers in Systems Neuroscience, 7,* 44.

Duffau, H., Moritz-Gasser, S., & Mandonnet, E. (2014). A re-examination of neural basis of language processing: Proposal of a dynamic hodotopical model from data provided by brain stimulation mapping during picture naming. *Brain and Language, 131,* 1–10.

Ford, A., McGregor, K. M., Case, K., Crosson, B., & White, K. D. (2010). Structural connectivity of Broca's area and medial frontal cortex. *Neuroimage, 52,* 1230–1237.

Freedman, M., Alexander, M. P., & Naeser, M. A. (1984). Anatomic basis of transcortical motor aphasia. *Neurology, 34,* 409–417.

Fujii, M., Maesawa, S., Motomura, K., Futamura, M., Hayashi, Y., Koba, I., et al. (2015). Intraoperative subcortical mapping of a language-associated deep frontal tract connecting the superior frontal gyrus to Broca's area in the dominant hemisphere of patients with glioma. *Journal of Neurosurgery, 122,* 1390–1396.

Galantucci, S., Tartaglia, M. C., Wilson, S. M., Henry, M. L., Filippi, M., Agosta, F., et al. (2011). White matter damage in primary progressive aphasias: A diffusion tensor tractography study. *Brain, 134,* 3011–3029.

Garcea, F. E., Dombovy, M., & Mahon, B. Z. (2013). Preserved tool knowledge in the context of impaired action knowledge: Implications for models of semantic memory. *Frontiers in Human Neuroscience, 7,* 1–18.

Garcea, F. E., Kristensen, S., Almeida, J., & Mahon, B. Z. (2016). Resilience to the contralateral visual field bias as a window into object representations. *Cortex, 81,* 14–23.

Garcea, F. E., & Mahon, B. Z. (2014). Parcellation of left parietal tool representations by functional connectivity. *Neuropsychologia, 60,* 131–143.

Goodglass, H., Kaplan, E., & Barresi, B. (2001). *Boston Diagnostic Aphasia Examination–Third Edition (BDAE–3)*. Philadelphia, PA: Lipscott, Williams, & Watkins.

Gotts, S. J., Saad, Z. S., Jo, H. J., Wallace, G. L., Cox, R. W., & Martin, A. (2013). The perils of global signal regression for group comparisons: A case study of autism spectrum disorders. *Frontiers in Human Neuroscience, 7,* 356.

Graham, M. S., Drobnjak, I., & Zhang, H. (2015). Realistic simulation of artefacts in diffusion MRI for validating post-processing correction techniques. *Neuroimage, 125,* 1079–1094.

Grossman, M., Powers, J., Ash, S., McMillan, C., Burkholder, L., Irwin, D., et al. (2013). Disruption of large-scale neural networks in non-fluent/agrammatic variant primary progressive aphasia associated with frontotemporal degeneration pathology. *Brain and Language, 127,* 106–120.

Guenther, F. H. (1995). Speech sound acquisition, coarticulation, and rate effects in a neural network model of speech production. *Psychological Review, 102,* 594–621.

Hamberger, M. J., Seidel, W. T., Mckhann, G. M., Perrine, K., & Goodman, R. R. (2005). Brain stimulation reveals critical auditory naming cortex. *Brain, 128,* 2742–2749.

Herbet, G., Moritz-Gasser, S., Boiseau, M., Duvaux, S., Cochereau, J., & Duffau, H. (2016). Converging evidence for a cortico-subcortical network mediating lexical retrieval. *Brain, 139,* 3007–3021.

Hickok, G., & Poeppel, D. (2000). Towards a functional neuroanatomy of speech perception. *Trends in Cognitive Sciences, 4,* 131–138.

Hickok, G., & Poeppel, D. (2007). The cortical organization of speech processing. *Nature Reviews Neuroscience, 8,* 393–402.

Hiroshima, S., Anei, R., Murakami, N., & Kamada, K. (2014). Functional localization of the supplementary motor area. *Neurologia Medico-Chirurgica, 54,* 511–520.

Howard, D., & Patterson, K. (1992). *Pyramids and Palm Trees: A test of semantic access from pictures and words*. Bury St. Edmunds, UK: Thames Valley Test Company.

Jellison, B. J., Field, A. S., Medow, J., Lazar, M., Salamat, M. S., & Alexander, A. L. (2004). Diffusion tensor imaging of cerebral white matter: A pictorial review of physics, fiber tract anatomy, and tumor imaging patterns. *American Journal of Neuroradiology, 25,* 356–369.

Jenkinson, M., & Smith, S. (2001). A global optimisation method for robust affine registration of brain images. *Medical Image Analysis, 5,* 143–156.

Kay, J., Coltheart, M., & Lesser, R. (1992). *PALPA: Psycholinguistic assessments of language processing in aphasia*. Hove, UK: LEA.

Kemerdere, R., de Champfleur, N. M., Deverdun, J., Cochereau, J., Moritz-Gasser, S., Herbet, G., et al. (2016). Role of the left frontal aslant tract in stuttering: A brain stimulation and tractographic study. *Journal of Neurology, 263,* 157–167.

Kim, J. H., Lee, J. M., Jo, H. J., Kim, S. H., Lee, J. H., Kim, S. T., et al. (2010). Defining functional SMA and pre-SMA subregions in human MFC using resting state fMRI: Functional connectivity-based parcellation method. *Neuroimage, 49,* 2375–2386.

Kinoshita, M., de Champfleur, N. M., Deverdun, J., Moritz-Gasser, S., Herbet, G., & Duffau, H. (2014). Role of fronto-striatal tract and frontal aslant tract in movement and speech: An axonal mapping study. *Brain Structure and Function, 220,* 3399–3412.

Klein, J. C., Behrens, T. E. J., Robson, M. D., Mackay, C. E., Higham, D. J., & Johansen-Berg, H. (2007). Connectivity-based parcellation of human cortex using diffusion MRI: Establishing reproducibility, validity and observer independence in BA 44/45 and SMA/pre-SMA. *Neuroimage, 34,* 204–211.

Krainik, A., Lehéricy, S., Duffau, H., Capelle, L., Chainay, H., Cornu, P., et al. (2003). Postoperative speech disorder after medial frontal surgery role of the supplementary motor area. *Neurology, 60,* 587–594.

Kristensen, S., Garcea, F. E., Mahon, B. Z., & Almeida, J. (2016). Temporal frequency tuning reveals interactions between dorsal and ventral visual streams. *Journal of Cognitive Neuroscience, 28,* 1295–1302.

Kronfeld-Duenias, V., Amir, O., Ezrati-Vinacour, R., Civier, O., & Ben-Shachar, M. (2016). The frontal aslant tract underlies speech fluency in persistent developmental stuttering. *Brain Structure and Function, 221,* 365–381.

Laplane, D., Talairach, J., Meininger, V., Bancaud, J., & Orgogozo, J. M. (1977). Clinical consequences of corticectomies involving the supplementary motor area in man. *Journal of the Neurological Sciences, 34,* 301–314.

Lawes, I. N. C., Barrick, T. R., Murugam, V., Spierings, N., Evans, D. R., Song, M., et al. (2008). Atlas-based segmentation of white matter tracts of the human brain using diffusion tensor tractography and comparison with classical dissection. *Neuroimage, 39,* 62–79.

Leng, B., Han, S., Bao, Y., Zhang, H., Wang, Y., Wu, Y., et al. (2016). The uncinate fasciculus as observed using diffusion spectrum imaging in the human brain. *Neuroradiology, 58,* 595–606.

Mahon, B. Z., Kumar, N., & Almeida, J. (2013). Spatial frequency tuning reveals interactions between the dorsal and ventral visual systems. *Journal of Cognitive Neuroscience, 25,* 862–871.

Mandelli, M. L., Caverzasi, E., Binney, R. J., Henry, M. L., Lobach, I., Block, N., et al. (2014). Frontal white matter tracts sustaining speech production in primary progressive aphasia. *Journal of Neuroscience, 34,* 9754–9767.

Mandonnet, E., Nouet, A., Gatignol, P., Capelle, L., & Duffau, H. (2007). Does the left inferior longitudinal fasciculus play a role in language? A brain stimulation study. *Brain, 130,* 623–629.

Oppenheim, G. (2017). A blind spot in correct naming latency analyses. *Cognitive Neuropsychology, 34,* 33–41.

Papagno, C., Miracapillo, C., Casarotti, A., Romero Lauro, L. J., Castellano, A., Falini, A., et al. (2010). What is the role of the uncinate fasciculus? Surgical removal and proper name retrieval. *Brain, 134,* 405–414.

Paul, D. A., Gaffin-Cahn, E., Hintz, E. B., Adeclat, G. J., Zhu, T., Williams, Z. R., et al. (2014). White matter changes linked to visual recovery after nerve decompression. *Science Translational Medicine, 6,* 266ra173.

Peeva, M. G., Guenther, F. H., Tourville, J. A., Nieto-Castanon, A., Anton, J. L., Nazarian, B., et al. (2010). Distinct representations of phonemes, syllables, and supra-syllabic sequences in the speech production network. *Neuroimage, 50,* 626–638.

Rozanski, V. E., Peraud, A., & Noachtar, S. (2015). Anomia produced by direct cortical stimulation of the pre-supplementary motor area in a patient undergoing preoperative language mapping. *Epileptic Disorders, 17,* 184–187.

Schnur, T. (2017). Word selection deficits and multiword speech. *Cognitive Neuropsychology, 34,* 21–25.

Sierpowska, J., Gabarrós, A., Fernandez-Coello, A., Camins, A., Castañer, S., Juncadella, M., et al. (2015). Morphological derivation overflow as a result of disruption of the left frontal aslant white matter tract. *Brain and Language, 142,* 54–64.

Smith, S. M. (2002). Fast robust automated brain extraction. *Human Brain Mapping, 17,* 143–155.

Snodgrass, J., & Vanderwart, M. (1980). A standardized set of 260 pictures: Norms for name agreement, image agreement, familiarity, and visual complexity. *Journal of Experimental Psychology: Human Learning and Memory, 6,* 174–215.

Song, S. K., Sun, S. W., Ramsbottom, M. J., Chang, C., Russell, J., & Cross, A. H. (2002). Dysmyelination revealed through MRI as increased radial (but unchanged axial) diffusion of water. *Neuroimage, 17,* 1429–1436.

Sonty, S. P., Mesulam, M., Thompson, C. K., Johnson, N. A., Weintraub, S., Parrish, T. B., et al. (2003). Primary progressive aphasia: PPA and the language network. *Annals of Neurology, 53,* 35–49.

Stasenko, A., Garcea, F., Dombovy, M., & Mahon, B. (2014). When concepts lose their color: A case of object-color knowledge impairment. *Cortex, 58,* 217–238.
Talairach, J., & Tournoux, P. (1988). *Co-planar stereotaxic atlas of the human brain. 3-Dimensional proportional system: An approach to cerebral imaging*. New York: Thieme.
Thiebaut de Schotten, M., Dell'Acqua, F., Valabregue, R., & Catani, M. (2012). Monkey to human comparative anatomy of the frontal lobe association tracts. *Cortex, 48,* 82–96.
Thomas, C., Avidan, G., Humphreys, K., Jung, K., Gao, F., & Behrmann, M. (2009). Reduced structural connectivity in ventral visual cortex in congenital prosopagnosia. *Nature Neuroscience, 12,* 29–31.
Tournier, J. D., Mori, S., & Leemans, A. (2011). Diffusion tensor imaging and beyond. *Magnetic Resonance in Medicine, 65,* 1532–1556.
Tourville, J. A., & Guenther, F. H. (2011). The DIVA model: A neural theory of speech acquisition and production. *Language and Cognitive Processes, 26,* 952–981.
Tremblay, P., & Gracco, V. L. (2009). Contribution of the pre-SMA to the production of words and non-speech oral motor gestures, as revealed by repetitive transcranial magnetic stimulation (rTMS). *Brain Research, 1268,* 112–124.
Tremblay, P., & Gracco, V. L. (2010). On the selection of words and oral motor responses: Evidence of a response-independent fronto-parietal network. *Cortex, 46,* 15–28.
Tremblay, P., & Small, S. L. (2011). Motor response selection in overt sentence production: A functional MRI study. *Frontiers in Psychology, 2,* 253.
Vassal, F., Boutet, C., Lemaire, J.-J., & Nuti, C. (2014). New insights into the functional significance of the frontal aslant tract—An anatomo-functional study using intraoperative electrical stimulations combined with diffusion tensor imaging-based fiber tracking. *British Journal of Neurosurgery, 28,* 685–687.
Vergani, F., Lacerda, L., Martino, J., Attems, J., Morris, C., Mitchell, P., et al. (2014). White matter connections of the supplementary motor area in humans. *Journal of Neurology, Neurosurgery & Psychiatry, 85,* 1377–1385.
Wakana, S., Caprihan, A., Panzenboeck, M. M., Fallon, J. H., Gollub, R. L., Hua, K., et al. (2007). Reproducibility of quantitative tractography methods applied to cerebral white matter. *Neuroimage, 36,* 630–644.